10(2013) 1243 – 1266

Latin American Journal of
Solids and Structures
www.lajss.org

Dynamic response of functionally graded skew shell panel

Abstract

The dynamic response of functionally graded skew shell is investigated using a C_0 finite element formulation. Reddy's higher order theory has been employed to perform the analysis and the volume fractions of the ceramic and metallic components are assumed to follow simple linear distribution law. The present study attempts to focus mainly on the influence of skew angle on frequency parameter and displacement of shell panel with various geometries. Comprehensive numerical results are demonstrated for cylindrical, spherical and hypar shells for different boundary conditions and skew angles.The findings obtained for functionally graded skew shell panels are new and can be used as bench mark for researchers in this field.

Keywords
Skew shell, functionally graded material, finite element formulation, higher order shear deformation theory.

**GulshanTaj M.N.A*
AnupamChakrabarti**

Departmentof Civil Engineering, IndianInstituteof Technology,
Roorkee-247 667, India.

Received 03 Dec 2012
In revisedform 01 Mar 2013

* Author email: gulshantaj19@yahoo.co.in

1 INTRODUCTION

Due to commodious applications of functionally graded material (FGM) in various fields of engineering, it enthralled the attention of many researchers worldwide. Moreover, the smooth and continuous change of mechanical properties across the preferred direction made them to occupy forefront in the material research. Understanding the vibration characteristics and dynamic behavior of members made of such materials is of prime importance from structural design point of view.

Owing to the above reasons, a large number of works have been devoted to conceive the vibration characteristics and dynamic response of functionally graded plates and shells exposed to thermo-mechanical loads. Consequently, many theories were developed to model the structure that accurately predicts its response under different loading environment. Some of the most widely adopted theories available in the scientific literature include first order shear deformation theory [26] and higher order shear deformation theory [24, 25]. In the past years, first order shear deformation theory (FSDT) which neglects the effects of transverse shear strain is used to accomplish the linear as well as non linear response of shells. For example, Zhao et al.[6] carried out static and vibration analysis of functionally graded cylindrical shell using element-free kp-Ritz method and found that the volume fraction exponent plays significant role in predicting the response of the shell; Kim et al. [4] presented the nonlinear analysis of FGM plates and shells using analytical solution and assumes the properties in terms of volume fraction exponent that follows sigmoid function; Arciniega and Reddy [3] presented a tensor based finite element formulation for large deformation analysis of FGM shells; and Reddy and Chin [10] examined the dynamic response of functionally graded plates and shells under thermo-mechanical environment. But the use of FSDT depends on the shear correction factor which is the cumbersome one to decide. Moreover, the theory may not be accurate in case of thick shells.

To explicate the shortcomings of the first order shear deformation theory many higher order shear deformation theories (HSDT) were developed in due course of time. It is noteworthy to mention that, Reddy's higher order shear deformation theory [24] is the most widely implemented by many researchers, where the realistic parabolic variation of transverse shear strain has been taken into account to eliminate the use of shear correction factor. Here, we cite the papers where the higher order theory [24]is successfully implemented with some analytical tools. Yang and Shen [18] analyzed the effect of thermal field on free and forced vibration analysis of functionally graded plates that combines the Reddy's higher order shear deformation plate theory with Galerkin technique. The plates with properties in between ceramic and metal components do not show the intermediate response, when the properties are considered as temperature dependent. Static and dynamic response of functionally graded plates using meshless local petrov-Galerkin approach in conjunction with higher order theory has been done by Qian et al.[19]. Mori-Tanaka method that includes interactions between various elastic constants is used to estimate the properties of the functionally graded plate. Neves et al. [14] extended the Carrera's unified formulation to perform vibration analysis of cylindrical shells. Two cases of transverse displacement (constant transverse displacement and quadratic variation with thickness coordinate) are considered to determine the frequency parameter of the cylindrical shell panels. Isvandzibaei and Moarrefzadeh[5] performed the free vibration analysis of FGM shells and influence of different parameters on frequency characteristics of shell are discussed briefly. Yang and Shen[15] examined the free vibration and stability analysis of FGM cylindrical shell panels under thermal and mechanical loads. Reddy's higher order theory, Galerkin technique and Blotin's method are applied to study the response of the shell panels under static and periodic loads. Setareh and Isvandzibaei[8] studied the vibration characteristics of functionally graded cylindrical shell using Reddy's higher order shear deformation theory. Influence of constituent volume fraction on frequency parameter was studied using Nickel and stainless steel shell panels. Pradyumna and Bandyopadhyay[13] located the unstable regions in functionally graded shell panels with different geometry (cylindrical, spherical, hypar and conical) using finite element formulation.

Other studies include the dynamic response and stability analysis of functionally graded shells by various numerical techniques. Ng et al. [9] carried out the stability analysis of FGM cylindrical shells using Bolotin's method. It is mentioned that control over the response of the plate can be achieved by proper variation of volume fraction exponent. Dynamic response of FGM shell under point load was investigated by Han et al.[12]. Nezhadi and Ayob [1] studied the dynamic response of the functionally graded cylindrical shell using Rayleigh-Ritz technique. Moreover, studies pertaining to special cases like shells embedded with piezoelectric layers are also considerable in number. Among them are: Wu and Syu[11], who studied the static response of functionally graded piezoelectric shells; and Alibeigloo et al.[7], who analyzed the free vibration of functionally graded piezo shells. On the whole, it can be interpreted that functionally graded materials are widely used in diverse fields of engineering, where situations like structural elements subjected to ultra high temperatures and sudden change in temperature within a fraction of seconds are encountered. Despite of high cost of this material which is considered as a drawback, proper design and tailoring of such material to suit different requirement made them to stand in the row of advanced materials.

To date, vibration and dynamic solution of functionally graded shell panels are limited to rectangular plan form only. Hence, an attempt is made to fill the apparent void exists in the literature by presenting the finite element solution to non rectangular plan form such as skew shells which have wide range of applications in modern construction industry. Reddy's higher order shear deformation theory [24] which satisfies the condition of zero transverse shear stress at top and bottom of the shell is implemented. The formulation also incorporates the term for twist curvature ($1/R_{xy}$) which plays a vital role to analyze the special forms like hypar shell, which is not yet done in any other formulation that incorporates Reddy's higher order theory. The present study is divided into two parts. The first part gives deep insight about the vibration characteristics of various forms of functionally graded skew shells (cylindrical, spherical and hypar) by incorporating different parameters such as skew angle *(a)*, thickness ratio (a/h), curvature ratio (R/a) and boundary conditions (simply supported and clamped). In the second part, dynamic response of skew shell is performed using Newmark integration scheme [16]. It is anticipated that the present results paves the way for researchers who are involved in the area of functionally graded skew shells.

2 MODELING AND FORMULATION

2.1 Shell geometry

A shell element having skew boundary with Cartesian coordinate system is depicted in Fig.1. The mid surface of the shell is assumed as origin for the material coordinate system. The top surface of the shell ($z=+h/2$) is rich in ceramic content, whereas the bottom surface of the shell ($z=-h/2$) is rich in metal content. A nine noded isoprametric Lagrangian shell element (Fig. 2) having seven nodal unknowns is employed to model the present shell element. For analysis of skew shells, the edges of the boundary elements are not parallel to the global axes (x, y) of the shell. Hence it is required to carry out the necessary transformation from global axes to local axes by using nodal transformation matrix $[T]$.For the shell finite element used in the present study the following transformation matrix $[T]$is utilized.

$$[T]=\begin{pmatrix} \cos\alpha & -\sin\alpha & 0 & 0 & 0 & 0 & 0 \\ \sin\alpha & \cos\alpha & 0 & 0 & 0 & 0 & 0 \\ 0 & 0 & 1 & 0 & 0 & 0 & 0 \\ 0 & 0 & 0 & \cos\alpha & -\sin\alpha & 0 & 0 \\ 0 & 0 & 0 & \sin\alpha & \cos\alpha & 0 & 0 \\ 0 & 0 & 0 & 0 & 0 & \cos\alpha & -\sin\alpha \\ 0 & 0 & 0 & 0 & 0 & \sin\alpha & \cos\alpha \end{pmatrix} \tag{1}$$

where α is the skew angle of the shell. For the elements which does not lies on skew edges no transformation will be required. For hypar shells, the surface equation can be expressed in the following manner. It should be noted that the ratio c/a implies the twist curvature for hypar shell.

$$z = 4\frac{c}{ab}xy + \frac{cx}{a} + \frac{cy}{b} \tag{2}$$

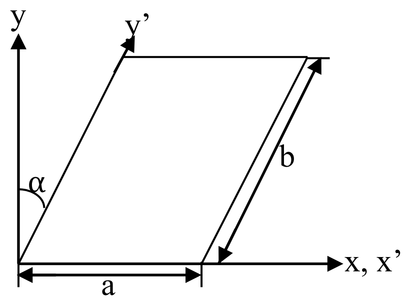

Figure 1 Plan view of FGM skew shell.

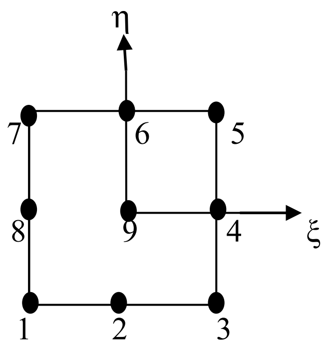

Figure 2 IsoparametricLagrangian element in natural co-ordinate system.

2.2 Effective properties of shell

Due to the dissimilarity of material properties along certain direction, it is necessary to evaluate the properties accurately using suitable method. Different schemes were proposed in the literature and some of them are: three phase model of Frohlich and Sack [20]; self consistent scheme [21]; Mori-Tanaka technique [22]; mean field approach [23]; Voigt method; and the representative volume element. Most widely adopted methods in the literature are Mori-Tanaka technique and Voigt method. In the present study Voigt method is employed to estimate the effective properties, such as, Young's modulus (E), Poisson's ratio (γ) and mass density (ϱ) of the shell panel as a function of position.

Based on the linear distribution law, effective properties of the shell constituents (E, γ and ϱ) are expressed in terms of volume fraction of the ceramic and metal content as mentioned below.

$$
\begin{aligned}
E(z) &= \left\{E_t - E_b\right\}\left(\frac{z}{h}+\frac{1}{2}\right)^n + E_b \\
\gamma(z) &= \left\{\gamma_t - \gamma_b\right\}\left(\frac{z}{h}+\frac{1}{2}\right)_c^n + \gamma_b \\
\rho(z) &= (\rho_t - \rho_b)\left(\frac{z}{h}+\frac{1}{2}\right)^n + \rho_b
\end{aligned}
\tag{3}
$$

where the subscripts "*t*" and "*b*" refers to the top and bottom of the surface of the shell respectively, n is the non-negative key parameter that describes the optimum distribution of constituents along the thickness direction of the shell. It takes the value between zero and infinity (i.e., zero corresponds to ceramic portion and infinity corresponds to metal portion). Since the variation of Poisson's ratio is negligible, it is assumed as constant in the present analysis.

The constitutive relationship of functionally graded shell may be written as,

$$
\begin{Bmatrix} \sigma_{xx} \\ \sigma_{yy} \\ \sigma_{yz} \\ \sigma_{xz} \\ \sigma_{xy} \end{Bmatrix} = \begin{bmatrix} Q_{11} & Q_{12} & 0 & 0 & 0 \\ Q_{21} & Q_{22} & 0 & 0 & 0 \\ 0 & 0 & Q_{33} & 0 & 0 \\ 0 & 0 & 0 & Q_{44} & 0 \\ 0 & 0 & 0 & 0 & Q_{55} \end{bmatrix} \begin{Bmatrix} \varepsilon_{xx} \\ \varepsilon_{yy} \\ \gamma_{yz} \\ \gamma_{xz} \\ \gamma_{xy} \end{Bmatrix}
\tag{4}
$$

where Q_{ij} contains the terms elastic moduli (E) and Poisson's ratio (γ), in which E alone is the function of depth as given below.

$$
Q_{11} = Q_{22} = \frac{E(z)}{1-\gamma^2},\ Q_{12} = Q_{21} = \frac{\gamma E(z)}{1-\gamma^2},\ Q_{44} = Q_{55} = \frac{E(z)}{2(1+\gamma)}
$$

Here, the Young's modulus (E) and Poisson's ratio (γ) of the panel at any height (z) of the shell can be easily estimated by using Equation (3). It should be noted that, the term $\left(\frac{z}{h}+\frac{1}{2}\right)^n$ involving in Equation (3) implies the volume fraction of the ceramic content (V_c) present in the panel considered. Further, the correlation between the volume fraction of ceramic (V_c) and metal (V_m) components is given by the relation $V_c+V_m=1.0$.

2.3 Displacement field

To describe the deformation profile of the shell panel, a special form of displacement field proposed by Reddy [24] is chosen, where the in-plane displacement fields (u and v) are expanded as cubic functions of the thickness coordinate (z), while the transverse displacement(w) variable has been assumed to be constant through the thickness. Any other choice of displacement field would either not satisfy the stress-free boundary conditions or lead to a theory that would involve more dependent unknowns than those in the first-order shear deformation theory [24]. Also, the theory leads to the parabolic distribution of transverse shear stresses and therefore the need of shear correction co-efficient could be avoided. According to Reddy's higher order shear deformation theory [24], the in-plane displacements (u and v) and transverse displacement (w) are expressed in terms of corresponding displacements at the mid surface (u_o, v_o and w_o) by the following expression.

$$\begin{aligned} u(x,y,z) &= u_0(x,y) + z\theta_x(x,y,z) + z^2\xi_x(x,y,z) + z^3\zeta_x(x,y,z) \\ v(x,y,z) &= v_0(x,y,z) + z\theta_y(x,y,z) + z^2\xi_y(x,y,z) + z^3\zeta_y(x,y,z) \\ w(x,y) &= w_0(x,y) \end{aligned} \tag{5}$$

where u, v and w are the displacements of any general point in the shell. The parameters u_0, $v_0$and w_0 are the displacements of points which are in the mid-surface (i.e., reference surface) of the shell and ϑ_x, ϑ_y are the bending rotations defined at the mid-surface about the y and x axes respectively. ξ_x, ξ_y, ζ_x and ζ_y are higher order terms appears in Taylor's series expansion and solved by the condition of zero transverse shear stains ($\gamma_{xz}(x,y,\pm h/2) = \gamma_{yz}(x,y,\pm h/2)=0$) at the top and bottom of the shell surface. Thus, incorporation of the above condition in Equation (5) leads to the expression for unknown higher order terms (ξ_x, ξ_y, ζ_x and ζ_y). Finally, by substituting the values of unknown higher order terms (ξ_x, ξ_y, ζ_x and ζ_y) in Equation (5) and rearranging all the terms that appears in the displacement field (u and v), the following final expression may be obtained.

$$\begin{aligned} u(x,y,z) &= u_0(x,y,z) + z\theta_x(x,y,z) - \frac{4z^3}{3h^2}\left(\theta_x + \frac{\partial w}{\partial x}\right) \\ v(x,y,z) &= v_0(x,y,z) + z\theta_y(x,y,z) - \frac{4z^3}{3h^2}\left(\theta_y + \frac{\partial w}{\partial y}\right) \\ w(x,y) &= w_0(x,y) \end{aligned} \tag{6}$$

In Equation (6), it is to be noted that the in-plane displacement field u and v invites the problem of C_1 continuity by the presence of second order derivatives in the strain part. The problem of choosing C_1 elements are well known due to its practical applications. In order to overcome the problem of C_1 continuity requirement at the time of finite element implementation the terms involving derivatives of transverse displacement are treated as separate field variables. i.e., $\psi_x^* = \left(\theta_x + \frac{\partial w}{\partial x}\right)$ and $\psi_y^* = \left(\theta_y + \frac{\partial w}{\partial y}\right)$

Hence by above substitution, the final in-plane displacement fields (u and v) for skew shell with the co-ordinate axes (x', y', z') can be modified as

$$\begin{aligned} u(x',y',z') &= u_o(x',y',z') + z\theta_x\left(1 - \frac{4z^2}{3h^2}\right) - \frac{4z^3}{3h^2}\psi_x^* \\ v(x',y',z') &= v_o(x',y',z') + z\theta_y\left(1 - \frac{4z^2}{3h^2}\right) - \frac{4z^3}{3h^2}\psi_y^* \end{aligned} \tag{7}$$

Hence, the basic field variables interpreted in the present study are u_0, v_0, w_0, ϑ_x, ϑ_y, ψ_{x^*} and ψ_{y^*} for each node thus forming a total of 63 nodal unknowns for the element.

2.4 Mathematical formulation

2.4.1 Strain displacement relation

All the formulation in the present study is confined to linear elastic behavior with small displacements and hence small strains. The linear strain- displacement relations according to Sander's shell theory are

$$
\begin{aligned}
\varepsilon_x &= \frac{\partial u}{\partial x} + \frac{w}{R_x} \\
\varepsilon_y &= \frac{\partial v}{\partial y} + \frac{w}{R_y} \\
\gamma_{xy} &= \frac{\partial u}{\partial y} + \frac{\partial v}{\partial x} + \frac{2w}{R_{xy}} \\
\gamma_{xz} &= \frac{\partial u}{\partial z} + \frac{\partial w}{\partial x} - \frac{C_1 u}{R_x} - \frac{C_1 v}{R_{xy}} \\
\gamma_{yz} &= \frac{\partial v}{\partial z} + \frac{\partial w}{\partial y} - \frac{C_1 v}{R_x} - \frac{C_1 u}{R_{xy}}
\end{aligned}
\tag{8}
$$

R_x, R_y represents the radii of curvature in the x and y directions respectively and R_{xy} is the twist radii of curvature. C_1 is the tracer that helps to reduce the approximation in to Love's shell theory and it is taken as unity in the present formulation. To combine equation (6), (7) and (8), the strain terms may be re-written as

$$
\begin{aligned}
\varepsilon_x &= \varepsilon_{xo} + z\left(1 - \frac{4z^2}{3h^2}\right)k_x - \frac{4z^3}{3h^2}k_x^* \\
\varepsilon_y &= \varepsilon_{yo} + z\left(1 - \frac{4z^2}{3h^2}\right)k_y - \frac{4z^3}{3h^2}k_y^* \\
\gamma_{xy} &= \gamma_{xyo} + z\left(1 - \frac{4z^2}{3h^2}\right)k_{xy} - \frac{4z^3}{3h^2}k_{xy}^* \\
\gamma_{yz} &= \phi_y + z\left(1 - \frac{4z^2}{3h^2}\right)k_{yz} - \frac{4z^3}{3h^2}k_{yz}^* - \frac{4z^2}{h^2}k_{yz}^{**} \\
\gamma_{xz} &= \phi_x + z\left(1 - \frac{4z^2}{3h^2}\right)k_{xz} - \frac{4z^3}{3h^2}k_{xz}^* - \frac{4z^2}{h^2}k_{xz}^{**}
\end{aligned}
\tag{9}
$$

where the different terms involved in the above equation are defined in the following fashion.

$$\left\{\varepsilon_{xo},\varepsilon_{yo},\gamma_{xyo}\right\}=\left\{\frac{\partial u_o}{\partial x}+\frac{w_o}{R_x},\frac{\partial v_o}{\partial y}+\frac{w_o}{R_y},\frac{\partial u_o}{\partial y}+\frac{\partial v_o}{\partial x}+\frac{2w_o}{R_{xy}}\right\}$$

$$\left\{\phi_x,\phi_y\right\}=\left\{\frac{\partial u}{\partial z}+\frac{\partial w}{\partial x}-\frac{C_1 u}{R_x}-\frac{C_1 v}{R_{xy}},\frac{\partial w}{\partial y}+\theta_y-\frac{C_1 v_o}{R_x}-\frac{C_1 u_o}{R_{xy}}\right\}$$

$$\left\{k_x,k_y,k_{xy},k_x^*,k_y^*,k_{xy}^*\right\}=\left\{\frac{\partial\theta_x}{\partial x},\frac{\partial\theta_y}{\partial y},\frac{\partial\theta_x}{\partial y}+\frac{\partial\theta_y}{\partial x},\frac{\partial\psi_x^*}{\partial x},\frac{\partial\psi_y^*}{\partial y},\frac{\partial\psi_x^*}{\partial y}+\frac{\partial\psi_y^*}{\partial x}\right\}$$

$$\left\{k_{xz},k_{yz},k_{xz}^*,k_{yz}^*,k_{xz}^{**},k_{yz}^{**}\right\}=\left\{\begin{array}{l}-C_1\dfrac{\theta_x}{R_x}-C_1\dfrac{\theta_y}{R_{xy}},-C_1\dfrac{\theta_y}{R_y}-C_1\dfrac{\theta_x}{R_{xy}},-C_1\dfrac{\psi_x^*}{R_x}-C_1\dfrac{\psi_y^*}{R_{xy}},\\ -C_1\dfrac{\psi_y^*}{R_y}-C_1\dfrac{\psi_x^*}{R_{xy}},\theta_x+\psi_x^*,\theta_y+\psi_y^*\end{array}\right\}$$

2.4.2 Free vibration analysis

The acceleration at any point within the element may be expressed in terms of the mid surface parameters (u_0, v_0 and w_0) as

$$\left\{\ddot{f}\right\}=\frac{\partial^2}{\partial t^2}\left\{\bar{f}\right\}=-\omega^2\begin{Bmatrix}u_0\\ v_0\\ w_0\end{Bmatrix}=-\omega^2\left[F\right]\left\{f\right\} \tag{10}$$

Where $\left\{f\right\}=\left[u_0\,v_0\,w_0\,\theta_x\,\theta_y\,\psi_x^*\psi_y^*\right]^T$ and the matrix $[F]$ contains the terms involving z and h as expressed below.

$$\left[F\right]=\begin{bmatrix}1&0&0&z&0&\dfrac{-4z^3}{3h^2}&0\\ 0&1&0&0&z&0&\dfrac{-4z^3}{3h^2}\\ 0&0&1&0&0&0&0\end{bmatrix}$$

Again the matrix $\{f\}$ is decoupled into matrix $[C]$ that contains the interpolation functions (N_i) and global displacement vector $\{X\}$.

$$\left\{f\right\}=\left[C\right]\left\{X\right\} \tag{11}$$

where the global displacement vector $\{X\}$ contains the nodal unknowns for all the nine nodes and thus forming the matrix of order 63x1. i.e., $\{X\}=\left[u_i\, v_i\, w_i\, \theta_x\, \theta_y\, \psi^*_{xi}\, \psi^*_{yi}\right]$, where i=1-9.

The shape functions in $[C]$ associated with the present nine noded Lagrangian element are as given below.

$$N_1=\frac{1}{4}(\xi-1)(\eta-1)\xi\eta, N_2=\frac{1}{4}(\xi+1)(\eta-1)\xi\eta, N_3=\frac{1}{4}(\xi+1)(\eta+1)\xi\eta,$$
$$N_4=\frac{1}{4}(\xi-1)(\eta+1)\xi\eta, N_5=-\frac{1}{2}\left(1-\xi^2\right)(1-\eta)\eta, N_6=-\frac{1}{2}(1+\xi)\left(\eta^2-1\right)\xi,$$
$$N_7=-\frac{1}{2}\left(\xi^2-1\right)(1+\eta)\eta, N_8=-\frac{1}{2}(\xi-1)\left(\eta^2-1\right)\xi, N_9=\left(1-\xi^2\right)\left(1-\eta^2\right).$$

Finally utilizing the Equations (10) and (11), the mass matrix of an element may be expressed as,

$$\left[m\right]=\iint_A\left[C\right]^T\left[L\right]\left[C\right]dA \tag{12}$$

where matrix $[L]$can be written as

$$\left[L\right]=\int_z\rho\left[F\right]^T\left[F\right]dz \tag{13}$$

Where ρ is the density of the material estimated from Equation (1). Hence the governing equation for free vibration analysis becomes,

$$\left(\left[K\right]-\omega^2\left[M\right]\right)\left\{X\right\}=\left\{0\right\} \tag{14}$$

where $[M]$, $[K]$ and ω are global mass matrix, global stiffness matrix and frequency parameter. The right hand side of the above equation zero represents the problem of free vibration analysis. Eigen value algorithm is utilized to extract the mode shapes of the shell panel.

2.5 Dynamic Response

For the problem of forced vibration Equation (14) is modified to incorporate damping matrix $[C]$ and the force vector $\{q\}$ at the right hand side. Hence the governing equation for forced vibration analysis becomes,

$$[M]\ddot{U}+[C]\dot{U}+[K]U=\{q\} \tag{15}$$

Where, $[M]$and $[K]$ represent the global mass matrix and stiffness matrix respectively.$[C]$ is the Rayleigh damping matrix and it is considered as below.

$$[C]=\alpha[M]+\beta[K] \tag{16}$$

In the above form, α and β are constants to be determined from two given damping ratios corresponding to two unequal frequencies of vibration. $\{q\}$appearing in Equation (12) is the dynamic pressure applied on the top of the shell. It is given by,

$$q(x,y,t)=q_0 F(t) \tag{17}$$

Here, q_0 is the maximum amplitude and F(t)is a dynamic load shape function of time domain. In the present analysis F(t) is taken as unity for the case of suddenly applied load. The extension of the linear acceleration method known as Newmark integration method [16] is used to obtain the transient response of the system. A step-by-step procedure for the problem of dynamic response is summarized below.

1. For the problem under consideration the stiffness matrix [K], mass matrix [M] and damping matrix [C]are formed as an initial step.
2. The magnitude of displacement$\left(U\right)$, velocity$\left(\dot{U}\right)$and acceleration$\left(\ddot{U}\right)$ at time t=0 are initialized.
3. The time step Δt is chosen, and parameters α and β are to be determined from damping ratios that corresponds to two unequal natural frequencies obtained from free vibration analysis.
4. The co-efficients are determined from the expression given below.

$$\begin{aligned} &a_o=\frac{1}{\alpha\Delta t^2};a_1=\frac{\beta}{\alpha\Delta t};a_2=\frac{1}{\alpha\Delta t};a_3=\frac{1}{2\alpha}-1;a_4=\frac{\beta}{\alpha}-1;\\ &a_5=\frac{\Delta t}{2}\left(\frac{\beta}{\alpha}-2\right);a_6=\Delta t(1-\beta);a_7=\delta\Delta t \end{aligned} \tag{18}$$

5. Effective stiffness matrix $[K']$ is formed as

$$[K']=[K]+a_0[M]+a_1[C] \tag{19}$$

6. The above formed effective stiffness matrix $[K']$ is triangularized. Then, effective loads $[R']$ are calculated at time t+Δt.
7. From the effective stiffness matrix $[K']$ and load matrix $[R']$ generated from step 5, the displacement is solved for time t+Δt and subsequently the velocity and acceleration can be estimated at time interval t+Δt.

3 DISCUSSION ON NUMERICAL PROBLEMS

This section is broken down into three parts: (1) The accuracy and efficiency of the present finite element formulation are validated with the existing literature data for free and forced vibration analysis; (2) Vibration analysis is done for skew shells with cylindrical ($R_x=R$, $R_y=R_{xy}=\infty$), spherical ($R_x=R_y=R$, $R_{xy}=\infty$) and hypar ($R_x=R_y=\infty$) geometry; and (3) Transient response of the cylindrical skew shell is studied under suddenly applied dynamic pressure. Properties of the ceramic and metal constituents adopted to perform these analyses are mentioned below.
FGM I: Silicon Nitride (Si_3N_4)/ Stainless steel (SUS_30_4):
E_c= 322.27GPa, E_m=207.78GPa, γ=0.3, ρ_c =2370, ρ_m = 8166.
FGM II: Silicon carbide (SiC)/ Aluminium (Al):
E_c= 427GPa, E_m=70 GPa, γ_c=0.17, γ=0.3, ρ_c =3210, ρ_m = 2707.
All the results presented herein are in non-dimensional forms and following are the different non-dimensional parameters implemented in the study.

Frequency: $\overline{\Omega} = \Omega a^2 \sqrt{12\rho_m(1-\gamma^2)/E_m h^2}$

Displacement: $\overline{w}(a/2, b/2) = \dfrac{w E_m h}{q_o a^2}$

Time: $\bar{t} = t\sqrt{E_m / a^2 \rho_m}$

Axial stresses: $\overline{\sigma_{xx}}(a/2, b/2) = \dfrac{\sigma_{xx} h^2}{q a^2}$

3.1 Free vibration analysis- validation study

The free vibration of FGM I cylindrical shell with simply supported boundary condition is demonstrated in Table 1. The mode shapes of first four frequencies for different power law exponent n = 0.0, 0.2, 2.0, 10.0 and 1000 (very high value), with geometric properties a/R=0.1 and a/h=10 are investigated. The source papers considered for comparison purposes are: Neves et al.[14], who adopted higher order shear deformation theory in conjunction with Carrera's unified formulation [28-30] and collocation radial basis techniques [31-34]; Pradyumna and Bandyobadyay [17], who presented free vibration solution using higher order shear deformation theory [25] combined with finite element formulation; and Yang and Shen [15], who carried out the vibration analysis using higher order shear deformation theory [27] and semi analytical approach. It may be concluded that the present results exhibit close range with the above cited reference data for the maximum number of cases.

Table 1 Vibration modes of square cylindrical shell (FGM I) with clamped boundary condition.

Power law exponent (n)	References	Mode 1	Mode 2	Mode 3	Mode 4
0.0 (Ceramic)	Present(12X12)[a]	74.503	142.647	142.816	201.072
	Yang and Shen [15]	74.518	144.663	145.740	206.992
	Pradyumna and Bandyopadhyay [17]	72.961	138.555	138.555	195.536
	Neves et al. [14]	74.263	141.677	141.848	199.156
0.2	Present (12X12)[a]	60.834	116.431	116.587	164.113
	Yang and Shen [15]	57.479	117.717	112.531	159.855
	Pradyumna and Bandyopadhyay [17]	60.026	113.880	114.026	160.623
	Neves et al. [14]	60.006	114.378	114.549	160.735
2.0	Present (12X12)[a]	40.585	77.356	77.451	108.754
	Yang and Shen [15]	40.750	78.817	79.407	112.457
	Pradyumna and Bandyopadhyay [17]	39.145	74.291	74.386	104.768
	Neves et al. [14]	40.525	76.972	77.081	107.948
10.0	Present (12X12)[a]	35.090	66.709	66.787	93.629
	Yang and Shen [15]	35.852	69.075	69.609	98.386
	Pradyumna and Bandyopadhyay [17]	33.366	63.286	63.366	89.197
	Neves et al. [14]	35.166	66.648	66.732	93.335
1000 (Metal)	Present (12X12)[a]	32.712	62.341	62.416	87.620
	Yang and shen [15]	32.761	63.314	63.806	90.370
	Pradyumna and Bandyopadhyay [17]	32.027	60.554	60.630	85.178
	Neves et al. [14]	32.610	61.932	62.008	86.816

[a] indicates mesh size

Maximum exception cases in first frequency mode are observed with Pradyumna and Bandyopadhyay[17] for the values of power law exponent n = 0.0, 2.0 and 10.0. The probable reason may be due to the different model of higher order theory involved in the reference paper by Pradyumna and Bandyopadhyay [17]. In case of Reddy's higher order deformation theory [24] used by the authors, the unknowns present in the in-plane displacement fields are determined by satisfying the condition of zero transverse shear stress at the top and bottom surface to be zero, which is not in the case of displacement field proposed by Kant and Khare [25]. Also, for higher modes, the results obtained by the present study shows slight deviation from the reference data. The different methods proposed to extract the frequencies may be the influence factor for this deviation amongst the results.

3.2. Dynamic response - validation study

The above formulation is extended to study the transient response of shell panel having different skew angles (a) and power law exponent (n). Validation part considers the square simply supported FGM ($Al/Zr0_2$) plate with geometric properties a $=b$ $=0.2$m and h=0.01m. The corresponding material properties are: E_c= 151GPa, γ_c =0.3, ρ_c =3000 kg/m^3 for Zirconia ($Zr0_2$) and E_m=70GPa, γ_m =0.3, ρ_m = 2707 kg/m^3 for Aluminium (Al). The plate is subjected to a uniformly distributed load of 10^6 N/m^2 in upward direction and time step of 0.00001s is considered. Fig.3 reveals the comparison of present results with those of Praveen and Reddy [2] which is based on first order shear deformation theory [35, 36]. The results are compared for selected values of power law exponent n = 0.0, 1.0 and 1000, again a good agreement between the results is observed for all the values of n considered.

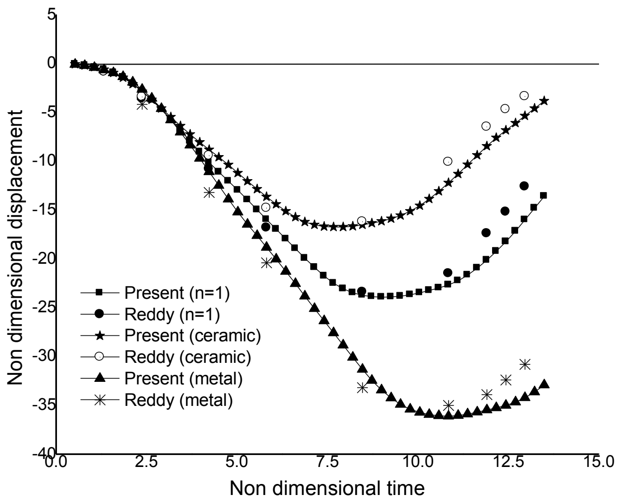

Figure 3 Transient response of plate (FGM I, simply supported) –Validation study.

3.3 New results

After examining the effectiveness of the present formulation, the study is extended to perform the vibration and dynamic analysis of FGM skew shells. The different shell forms such as cylindrical, spherical and hypar are considered to generate new results.

3.3.1 Skew cylindrical shell with various thickness ratios (*a*/*h*)

Table 2 present the non dimensional frequency of square clamped cylindrical skew shell with R/a =5.0 for several skew angles (a). Power law exponent (n) is varied from ceramic phase to metal phase according to Equation (1) to show its influence on frequency parameter. It is seen that, as the power law index rises, the frequency of the shell tends to reduce, which is also the most common observation in case of shells with no skew boundary. The low stiffness offered by the metal portion may be the contributing phenomenon for the above statement. Next, the increasing trend of the frequency with fall in thickness of the shell, due to dominance of mass effect is observed. Also, with the increase of skew angle of the shell (i.e., beyond skew angle 30°), the frequency parameter tends to increase at faster rate (nearly about 1.5-1.7 times). For thick shells (a/h =5.0 and 10.0) with clamped boundary and skew angle 30°, the deviation in results is found from other cases (a/h =20.0, 50.0 and 100). Therefore, it can be inferred that the present model will not accurately predict the frequency in case of thick clamped cylindrical skew shell predominantly for skew angle 30°. Fundamental frequency mode of simply supported cylindrical skew shell with R/a=5.0 and different values of power law exponent (n) are established in Table 3. As estimated, the clamped skew shell establish higher frequency compared to simply supported shell, due to high stiffness.

Table 2 Non dimensional frequencies of square cylindrical shell (FGM II) with clamped boundary condition (R/a=5.0).

a/h	Skew angle (a)	Power law exponent (n)							
		0	0.2	0.5	1.0	2.0	5.0	10	1000
5	15°	102.822	96.143	88.284	79.251	69.234	57.842	52.183	44.317
	30°	101.371	94.744	86.956	78.070	68.282	56.850	51.134	43.376
	45°	139.226	130.230	119.646	107.450	93.654	77.202	69.172	59.579
	60°	216.383	202.808	186.871	168.348	146.744	120.123	107.135	92.582
10	15°	185.024	171.999	156.798	140.145	122.578	103.601	94.044	80.083
	30°	171.945	160.384	147.136	132.399	116.610	98.979	89.621	75.080
	45°	242.460	226.300	207.582	186.537	163.679	137.670	124.185	104.825
	60°	395.899	370.347	340.463	306.286	267.921	222.554	199.645	170.403
20	15°	294.111	272.805	248.382	221.734	194.815	167.807	153.708	128.646
	30°	299.849	280.400	258.372	233.763	206.533	175.248	158.265	131552
	45°	417.148	389.657	358.343	323.420	285.271	242.099	218.796	181.977
	60°	697.837	652.297	599.751	540.624	475.672	401.239	361.731	303.170
50	15°	534.163	495.534	451.386	403.477	355.577	309.121	284.618	234.978
	30°	693.548	650.797	602.222	547.096	483.754	407.581	365.747	304.370
	45°	934.133	875.746	809.441	734.455	648.985	547.264	491.578	408.749
	60°	1523.040	1427.625	1318.461	1194.980	1055.548	891.609	802.190	667.230
100	15°	865.366	806.316	739.451	665.682	587.119	502.407	456.651	377.459
	30°	1358.464	1275.945	1181.824	1074.461	950.124	799.230	716.050	596.066
	45°	1813.851	1702.820	1576.456	1432.625	1266.382	1065.001	951.151	794.043
	60°	2897.804	2720.454	2517.364	2286.156	2021.261	1704.125	1529.640	1272.777

Table 3 Non dimensional frequencies of square cylindrical shell (FGM II) with simply supported boundary condition (R/a=5.0).

a/h	Skew angle	Power law exponent (n)							
	(a)	0	0.2	0.5	1.0	2.0	5.0	10	1000
5	15°	53.388	49.875	45.871	41.374	36.412	30.693	27.621	22.951
	30°	82.586	76.946	70.400	62.981	54.933	45.898	41.425	35.264
	45°	111.264	104.962	97.497	88.578	77.863	64.833	58.034	47.404
	60°	150.283	143.009	134.086	122.837	108.356	90.098	80.542	64.179
10	15°	96.784	90.395	83.172	75.010	66.196	55.974	50.420	41.895
	30°	138.752	128.777	117.872	105.667	92.876	79.113	71.918	60.337
	45°	213.801	200.471	185.021	167.208	147.081	123.628	110.968	91.572
	60°	294.951	278.867	260.227	238.182	211.245	176.641	156.895	125.992
20	15°	175.069	162.844	148.822	113.269	117.244	100.701	91.625	76.290
	30°	235.901	219.941	201.892	181.905	160.377	136.613	123.879	103.166
	45°	389.747	364.161	335.143	302.710	266.935	226.148	204.161	170.081
	60°	583.545	549.221	510.231	465.263	411.876	344.735	306.428	249.947
50	15°	343.732	319.794	292.993	263.615	232.321	198.385	180.275	149.982
	30°	510.505	476.861	438.863	396.507	349.894	297.010	268.362	223.337
	45°	888.385	831.905	767.856	695.661	614.205	518.860	467.049	389.619
	60°	1436.591	1354.542	1265.107	1132.626	996.447	835.543	746.387	612.483
100	15°	612.748	571.037	524.088	472.134	416.283	354.822	321.181	266.623
	30°	946.338	885.230	816.317	739.081	652.493	551.682	496.762	413.288
	45°	1706.310	1599.148	1473.810	1328.351	1170.123	995.443	896.831	745.520
	60°	2745.516	2569.263	2369.666	2145.473	1893.306	1597.616	1436.002	1190.948

3.3.2 Skew spherical shell with various thickness ratios (a/h)

The fundamental frequency of square spherical shell with clamped and simply supported boundary condition is demonstrated in Table 4 and Table 5, respectively. Shell panel with R/a=5.0 and several values of thickness ratio (a/h) are considered. The observations drawn for spherical shell are similar to those for cylindrical shells, except that high magnitude of frequency is reported in case of spherical shell.

Table 4 Non dimensional frequencies of square spherical shell (FGM II) with clamped boundary condition (R/a=5.0).

a/h	Skew angle (a)	Power law exponent (n)							
		0	0.2	0.5	1.0	2.0	5.0	10	1000
5	15°	118.769	113.112	106.350	98.089	87.605	73.178	64.509	49.865
	30°	134.209	127.982	120.436	111.092	99.095	82.544	72.829	56.552
	45°	167.197	160.012	151.073	139.545	124.008	102.785	91.109	70.799
	60°	231.432	221.269	207.937	189.837	165.221	136.131	122.957	98.608
10	15°	227.841	215.096	200.526	183.522	163.047	136.544	120.737	95.661
	30°	249.303	236.188	220.802	202.578	180.478	151.577	134.413	107.090
	45°	312.867	297.302	278.782	256.440	228.725	191.788	169.955	134.698
	60°	444.292	422.317	394.756	358.670	315.584	263.484	236.125	192.118
20	15°	433.195	407.757	378.694	345.208	305.885	256.928	228.714	185.795
	30°	481.982	453.905	421.762	384.733	341.196	286.645	255.106	206.980
	45°	601.828	567.741	528.306	482.473	428.321	360.064	320.420	259.052
	60°	841.972	790.077	729.640	660.709	583.011	491.312	441.658	368.184
50	15°	1055.636	990.086	916.386	833.110	737.080	619.584	552.284	453.260
	30°	1170.697	1098.825	1017.694	925.462	818.106	685.900	611.378	502.225
	45°	1437.485	1349.729	1250.066	1136.465	1004.953	844.381	753.608	618.200
	60°	1942.545	1824.688	1689.009	1534.186	1356.430	1143.033	1025.769	852.656
100	15°	2118.873	1982.404	1837.416	1681.582	1464.397	1218.010	1090.172	903.134
	30°	2320.251	2175.791	2013.102	1828.599	1614.298	1352.009	1205.708	994.916
	45°	2787.506	2611.840	2413.901	2190.306	1933.477	1623.580	1451.427	1197.823
	60°	3773.824	3546.135	3284.538	2985.526	2640.176	2222.549	1991.944	1654.534

Table 5 Non dimensional frequencies of square spherical shell (FGM II) with simply supported boundary condition (R/a=5.0).

a/h	Skew angle	Power law exponent (n)							
	(a)	0	0.2	0.5	1.0	2.0	5.0	10	1000
5	15°	70.435	67.100	62.922	58.004	52.453	44.708	39.451	29.896
	30°	91.233	87.173	82.240	76.273	68.905	58.169	51.061	38.501
	45°	116.113	110.950	104.671	96.866	86.682	72.269	63.682	49.182
	60°	151.826	145.167	136.969	126.514	112.545	93.545	82.937	64.716
10	15°	124.097	117.594	109.868	100.849	90.303	76.392	67.616	52.937
	30°	168.884	160.016	149.738	137.711	123.203	103.687	91.410	71.268
	45°	221.471	209.943	196.516	180.595	161.039	134.843	119.027	93.741
	60°	296.372	281.168	263.429	242.203	215.706	180.290	159.414	126.318
20	15°	231.618	218.506	203.273	185.670	165.132	139.185	123.701	99.292
	30°	325.842	306.822	285.331	260.683	231.492	194.069	171.782	137.498
	45°	427.999	402.915	374.433	341.676	303.036	254.031	225.219	180.925
	60°	585.131	551.643	513.447	469.126	416.014	347.946	308.485	249.207
50	15°	540.704	508.451	471.324	428.801	379.772	319.895	285.531	233.080
	30°	796.679	747.061	691.631	628.853	555.625	464.637	412.593	336.357
	45°	1031.472	966.306	893.666	811.658	716.652	599.803	533.327	435.128
	60°	1432.093	1343.148	1243.084	1129.401	997.463	835.317	743.462	608.399
100	15°	1032.021	969.501	897.736	815.787	721.629	607.790	543.353	446.232
	30°	1576.086	1475.905	1364.275	1238.315	1092.292	912.888	811.732	665.998
	45°	2033.259	1902.225	1756.954	1593.624	1404.795	1173.654	1043.847	857.016
	60°	2807.427	2627.588	2426.963	2200.913	1940.566	1624.170	1446.948	1189.335

3.3.3 Skew cylindrical and spherical shell with several curvature ratios (*R/a*)

This example refers to the square cylindrical and spherical shell with a/h=10, power law exponent n =1.0, having simply supported and clamped boundary condition. Various values of R/a ratio (0.2, 0.5, 5.0, 10.0, and 50.0) are selected to perform the study. Influence of R/a ratio on frequency parameter for cylindrical, spherical skew shell with simply supported and clamped boundary condition are investigated in Fig.4 and Fig.5, respectively. It should be noted that, R=1/radius of curvature is adopted in this case. Up to a certain value of R/a (i.e.,(R/a)=2.0), it endures decline tendency in hasty manner, after which it converges to a constant for all the values of R/a considered. The shell with clamped boundary confirms elevated frequency compared to shell with simply supported boundary. Further-more, spherical skew shell authenticates its superiority over cylindrical skew shell irrespective of the value of R/a considered.

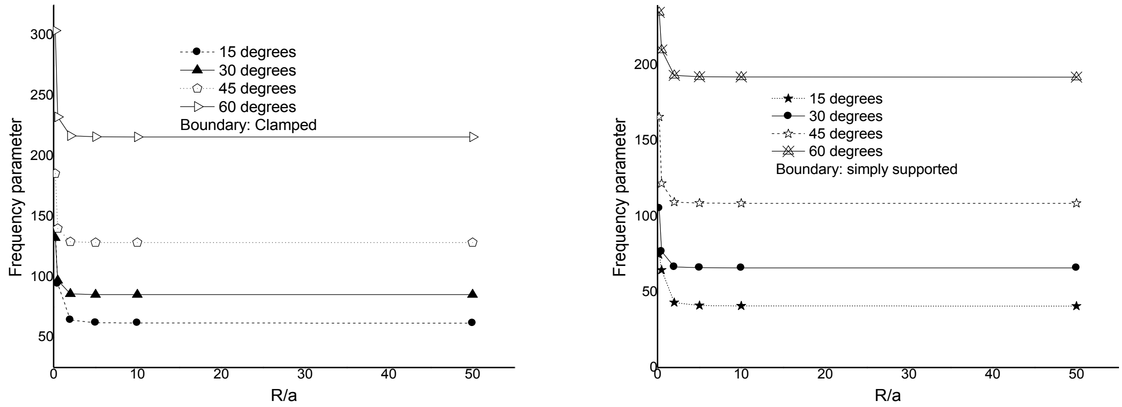

Figure 4 Influence of R/a ratio on non dimensional frequencies of cylindrical skew shell (FGM II, n =1.0, a/h=10).

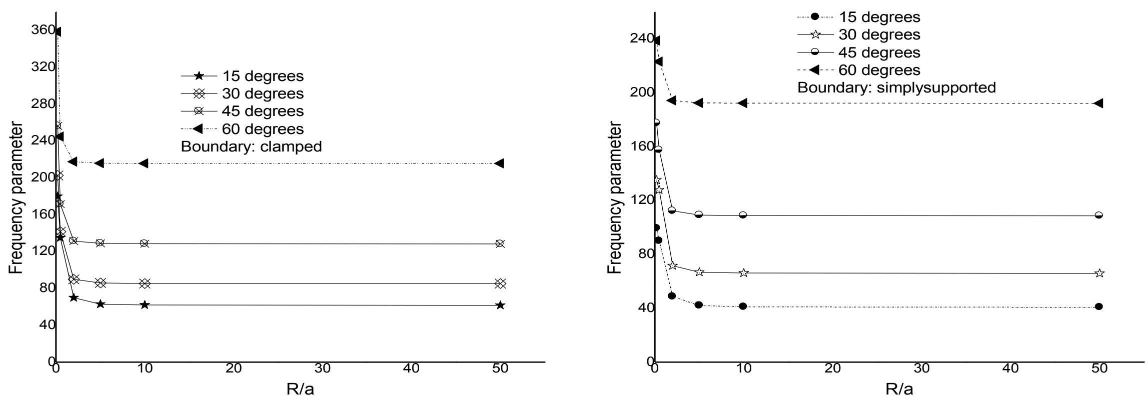

Figure 5Influence of R/a ratio on non dimensional frequencies of spherical skew shell (FGM II, n =1.0, a/h=10)

3.3.4 Skew hypar shell with various c/a ratios

In this example, the term c/a is used as an indicator of the twist curvature of hypar shell. Effect of c/a ratio on frequency parameter for simply supported and clamped boundary conditions having geometric properties $a/\ h$=10.0 and power law exponent (n)=1.0 is illustrated in Table 6. When the c/a ratio improves from 0.0 to 0.3, the frequency of the shell increases for all the skew angles (a) considered. As anticipated, shell with clamped boundary shows more frequency than shell with simply supported boundary.

Table 6 Non-dimensional frequencies of square hypar skew shell (FGM II, a/h =10.0, n =1.0)

Boundary condition	Skew angle (α)	c/a						
		0	0.05	0.1	0.15	0.2	0.25	0.3
Simply supported	15°	37.085	37.130	37.263	37.484	37.788	38.170	38.625
	30°	60.418	60.448	60.556	60.741	61.002	61.338	61.748
	45°	100.105	100.136	100.238	100.408	100.647	100.955	101.331
	60°	177.715	177.745	177.806	177.897	178.018	178.170	178.352
Clamped	15°	56.200	56.254	56.417	56.687	57.063	57.542	58.121
	30°	78.036	78.072	78.174	78.342	78.576	78.874	79.236
	45°	118.182	118.214	118.306	118.458	118.670	118.941	119.271
	60°	199.356	199.376	199.424	199.500	199.603	199.735	199.894

3.3.5 Cylindrical skew shell subjected to dynamic pressure

In order to generate new results for dynamic response of cylindrical (FGM I) skew shell the effects of different parameters such as skew angle (α), volume fraction index (n), shell geometry (cylindrical and spherical) and aspect ratio (b/a) are considered and the results are presented in the form of Figures (Figs. 6-9).Simply supported boundary condition is adopted to perform all the problems related to dynamic response of the panel and the displacement at the center of the shell is shown in all the figures. As a first illustration, in order to study the consequence of change of skew angle on the central displacement, cylindrical shell with a/h=10.0 is used and depicted in Fig.6. In this example, the value of the skew angle ranges from 15° to 60° and a linear variation of n (n=1.0) is considered. Cylindrical shell with skew angle 30° endures the maximum displacement; and the minimum displacement is observed for skew angle 60°. Hence it is concluded that, an increase in skew angle contributes more stiffness to the shell under consideration thus recording minimum displacement at the center of the shell. Fig.7 reveals the consequence of aspect ratio (b/a) on central displacement component for cylindrical shell with skew angle (α) =15°. Four different cases of aspect ratio (b/a= 0.5, 1.0, 2.0 and 5.0) and skew angle 15 °are chosen to perform the study. Smaller aspect ratio (b/a=0.5) ensures maximum central displacement while the minimum value is observed for the value of b/a=5.0. Shell with aspect ratio b/a=5.0 exhibits negligible displacement is also observed in Fig.7. In Fig. 8, skew shell (α =15°) with two different geometry namely, cylindrical and spherical shells are considered for the study. As expected, the spherical shell report less deflection compared to cylindrical shell, thus ensuring its high stiffness. Next, the power law exponent (n) is varied from ceramic (n=0) to metal segment (n=very high value), to study its influence on transient response of cylindrical skew shell as demonstrated in Fig. 9. Shell with pure metal (n=very high value) gives maximum displacement, followed by composite shell and pure ceramic shell (n=0.0). Dominance of stiffness effect offered by pure ceramic shell may be the possible cause for the above observation. At the end, variation of axial stresses over a period of time for cylindrical shell having skew angle 0° to 60° is also studied. The shell with skew angle (α) 30° gives maximum axial stress compared to other skew shells.

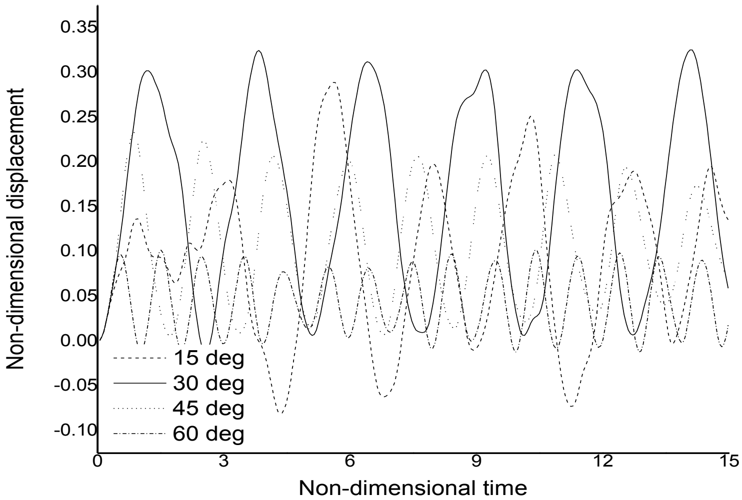

Figure 6 Influence of skew angle (α) on the transient response of cylindrical shell (FGM I, n =1.0, a/h=10.0)

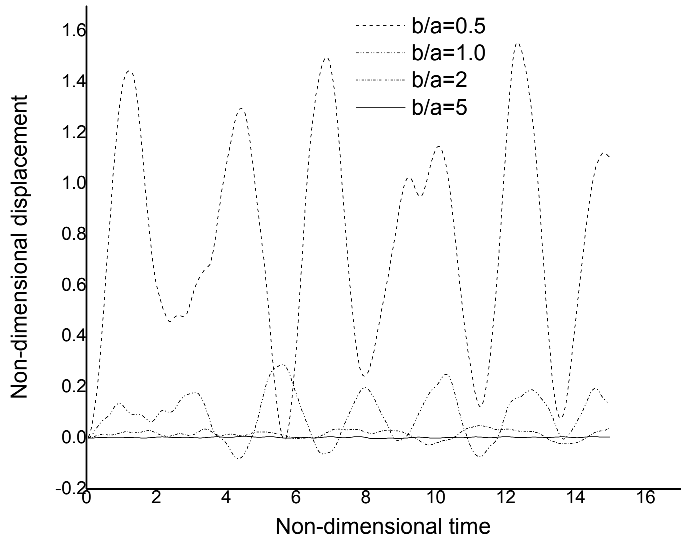

Figure 7 Effect of aspect ratio *(b/a)* on dynamic response of cylindrical skew shell (FGM I, α=15°, n=1.0, a/h=10.0)

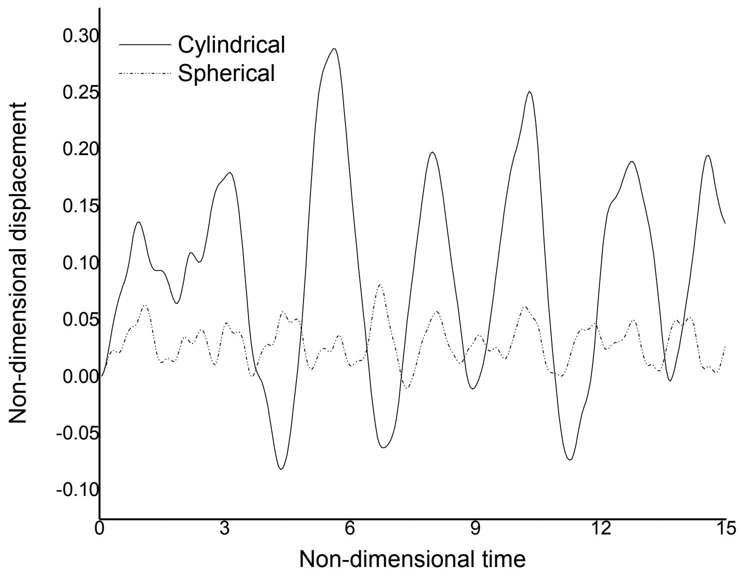

Figure 8 Influence of shell geometry on the dynamic response of cylindrical skew shell (FGM II, α =15°, n =1.0, a/h=10.0)

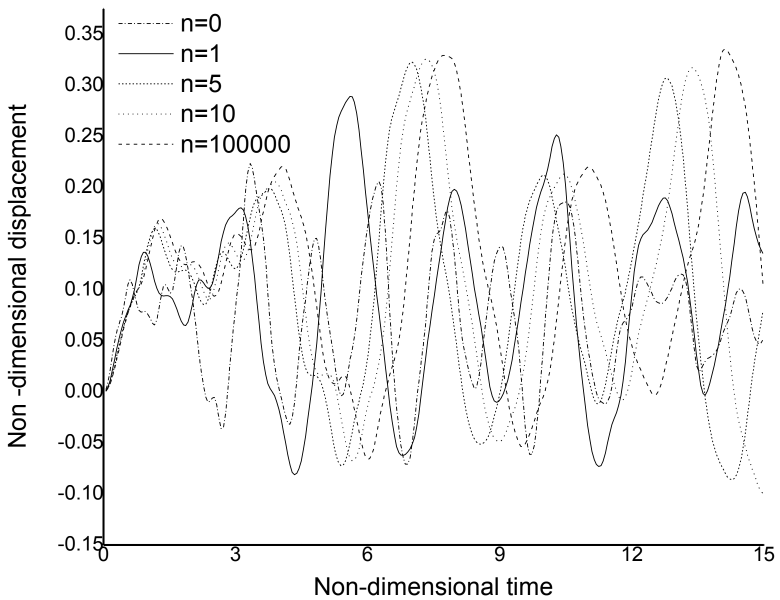

Figure 9 Influence of power law exponent (n) on the dynamic response of cylindrical skew shell (FGM II, α =15°, a/h=10.0)

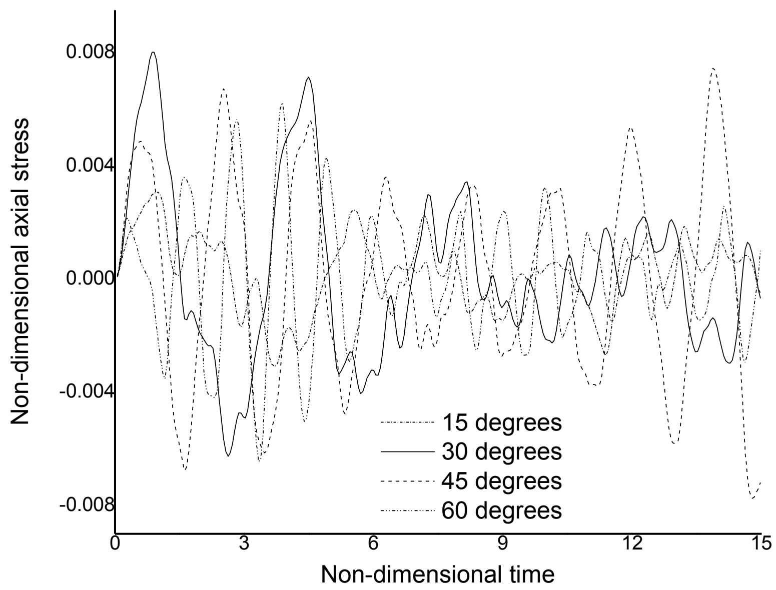

Figure 10 Influence of non-dimensional axial stresses on the dynamic response of cylindrical skew shell (FGM II, α =15°, n =1.0, a/h =100).

4 SUMMARY

In the present paper the dynamic response of functionally graded skew shell has been studied by using a C_0 finite element formulation which is developed to overcome the issue of C_1 continuity associated with the present higher order shear deformation theory (HSDT). Different types of skew shell geometries are considered and various conclusions regarding the analysis are highlighted in the discussion section. The term for twist curvature is also included in the formulation to analyze special shell forms such as hypar shells. Based on the detailed study, the following observations are drawn regarding the free and forced vibration response of different types of functionally graded shells by varying different geometric and material parameters.

i. **Skew angle:** Increase in skew angle (a) exhibit higher frequency irrespective of the value of powerlaw exponent (n) considered and hence ensures minimum displacement. Also, shell with skew angle 30° gives the maximum axial stress.

ii. **Shell geometry:** Spherical skew shell establish better performance in vibration and transient response compared to cylindrical skew shell when boundary condition and other parameters (i.e., geometric properties and power law exponent) are kept constant.

iii. **Boundary conditions:** Skew shell with clamped boundary shows higher frequency than shell with simply supported boundary, due to the high rigidity in the first case.

iv. **Other parameters:** Due to preponderance effect of either mass or stiffness, fundamental frequency tends to decrease with the (a) raise in curvature ratio (R/a) and (b)fall-off in thickness ratio (a/h) for all the skew angles assumed.

The above conclusions may be helpful for the researchers affianced in analysis and design of skew shell panels, as they are reported for the first time.

References

[1] Amirhossein Nezhadi, Roslan Abdul Rahman and Amran Ayob,(2011). Transient analysis of functionally graded cylindrical shell under impulse local loads, Australian J. Basic and Applied Sciences 5(12): 757-765.

[2] Praveen, G.N., and Reddy,J.N., (1998). Nonlinear transient thermoelastic analysis of functionally graded ceramic-metal plates, Int. J. Solids and Structures 35(33): 4457-4476.

[3] Arciniega, R.A., and Reddy, J.N., (2007). Large deformation analysis of functionally graded shells, Int. J. Solids and Structures 44: 2036-2052.

[4] Ki du kim, Gilson Rescober Lomboy and Sung Cheon Han, (2008) Geometrically non-linear analysis of functionally graded material plates and shells using a four node quasi conforming shell element, J. Composite Materials 42(5): 485-511.

[5] Mohammad Reza Isvandzibaei and Ali Moarrefzadeh, (2011). Vibration two type functionally graded cylindrical shell, Int. J. Multidisciplinary Sciences and Engineering 2(8): 7-11.

[6] Zhao, Lee, Y.Y., and Liew, K.M., (2009). Thermoelastic and vibration analysis of functionally graded cylindrical shells, Int. J. Mechanical Sciences 51: 694-707.

[7] Alibeigloo, A.,Kani, A.M., and Pashaei, M.H., (2012). Elasticity solution for the free vibration analysis of functionally graded cylindrical shell bonded to thin piezoelectric layers: Int. J. Pressure Vessels and Piping, 89: 98-111.

[8] Mohammed Setareh,A., and Mohammad Reza Isvandzibaei, (2011). A finite element formulation for analysis of functionally graded plates and shells, J. Basic and Applied Scientific Research 1(9): 1236-1243.

[9] Ng, T.Y., Lam, K.Y., Liew, K.M., and Reddy, J.N., (2001). Dynamic stability analysis of functionally graded cylindrical shells under periodic axial loading, Int. J. Solids and Structures 38: 2001, 1295-1309.

[10] Reddy, J.N., and Chin, C.D., (1998). Thermomechanical analysis of functionally graded cylinders and plates, J.of Thermal Stresses 21: 593-626.

[11] Chih-Ping Wu., and Yun-Siang Syu, (2007). Exact solutions of functionally graded piezoelectric shells under cylindrical bending, Int. J. Solids and Structures 44: 6450-6472.

[12] Han, X., and Xu, D., (2002). Transient responses in a functionally graded cylindrical shell to a point load, J. Sound and Vibration 251(5): 783-805.

[13] Pradyumna, S., and Bandyopadhyay, J.N., (2010). Dynamic instability of functionally graded shells using higher order theory, J. Engineering Mechanics 136: 551-561.

[14] Neves, A.M.A., Ferreira, A.J.M., Carrera, E., Cinefra, M., Roque, C.M.C., Jorge, R.M.N. and Soares, C.M.M., (2013). Free vibration analysis of functionally graded shells by a higher-order shear deformation theory and radial basis functions collocation, accounting for through-the-thickness deformations, Eur. J. Mechanics A/Solids 37: 24-34.

[15] Yang, J., Shen., and Hui-Shen, (2003). Free vibration and parametric resonance of shear deformable functionally graded cylindrical panels, J. Sound and Vibration 261(5): 871-893.

[16] Bathe, K.J., Ramm, E., and Wilson, E.L., (1975). Finite element formulations for large deformation dynamic analysis, Int. J. Numerical Methods in Engineering 9: 353-386.

[17] Pradyumna, S., and Bandyopadhyay, J.N., (2008). Free vibration analysis of functionally graded curved panels using a higher-order finite element formulation, J. Sound and Vibration 318: 176-192.

[18] Yang, J., and Shen, H.S., (2002). Vibration characteristics and transient response of shear-deformable functionally graded plates in thermal environments, J. Sound and Vibration 255(3): 579-602.

[19] Qian, L.F., Batra, R.C., and Chen, L.M., (2004). Static and dynamic deformations of thick functionally graded elastic plates by using higher-order shear and normal deformable plate theory and meshless local Petrov-Galerkin method, Composites: part B: 685-697.

[20] Frohlich, H., Sack, R., (1946). Theory of the rheological properties of dispersions. Proceedings of the royal society of London A 185: 415-430.

[21] Hill R., (1965). A self consistent mechanics of composite materials. J. Mechanics and Physics of Solids 13: 213-222.

[22] Mori, T., and Tanaka, K., (1973). Average stress in matrix and average elastic energy of materials with mis-fitting inclusions, Acta Metallurigca 21: 571-574.

[23] Jiang, B., and Batra, R.C., (2002). Effective properties of a piezo composite containing shape memory alloy and inert inclusions, Continuum Mechanics and Thermodynamics 14: 87-111.

[24] Reddy, J.N., (1984). A simple higher-order theory for laminated composite plate, J. Applied Mechanics 51: 745-752.

[25] Kant., and Khare, R.K, (1997). A higher-order facet quadrilateral composite shell element, Int. J. of Numerical Methods in Engineering 40: 4477-4499.

[26] Mindlin, R.D., (1951). Influence of rotary inertia and shear on flexural vibrations of isotropic elastic plates, J. Applied Mechanics 73: 31-38.

[27] Reddy, J.N., and Liu, C.F., (1985). A higher-order shear deformation theory of laminated elastic shells, Int. J. Engineering Science 23(3): 319-330.

[28] Carrera, E., (2001). Developments, ideas, and evaluations based upon Reissner's mixed variation theorem in the modeling of multilayered plates and shells, Applied Mechanics Reviews 54: 301-329.

[29] Carrera, E., (2003). Theories and finite elements for multilayered plates and shells: a unified compact formulation with numerical assessment and benchmarking. Archives of Computaional methods in engineering 10: 215-296.

[30] Carrera, E., (2004). On the use of murakami's zig-zag unction in the modeling of layered plates and shells, Computers and Structures 82: 541-554.

[31] Ferreira, A.J.M., (2003a). A formulation of the multiquadric radial basis function method for the analysis of laminated composite plates, Composite structures 59: 385-392.

[32] Ferreira, A.J.M., (2003b). Thick composite beam analysis using a global meshless approximation based on radial basis functions, Mechanics of Advanced Materials and Structures 10: 271-284.

[33] Ferreira, A.J.M., Roque, C.M.C., Martins, P.A.L.S., (2003). Analysis of composite plates using higher-order shear deformation theory and a finite point formulation based on the multiquadric radial basis function method. Composites: Part B 34: 627-636.

[34] Ferreira, A.J.M., Roque, C.M.C., Jorge, R.M.N., (2006). Analysis of composite and sandwich plate by trigonometric layer-wise deformation theory and radial basis function. J. Sandwich Structures and Materials 8: 497-515.

[35] Reddy, J.N., (1984b). Energy and Variational methods in Applied Mechanics, Wiley Interscience, New York.

[36] Reddy, J.N., (1997). Mechanics of laminated composite plates, Theory and Analysis, CRC press, Boca Raton, FL.